TIANWEN-1 LANDING SITE ATMOSPHERIC CONDITION BASED ON 2021 LOCAL DUST STORMS OF MARS

Abstract

The present study is based on the local dust storms reported by Tianwen-1. In the year 2021 Tianwen-1 reported 6 local dust storms near mid-latitude (*Qu et al., 2021*). The current work tries to investigate the atmospheric changes over the lendable area during the reported dust events by Tianwen-1. Based on the temperature profile acquired by Mars Climate Sounder (MCS), we have estimated the Convective Boundary Layer's (CBL) height. The estimated CBL height varies from 7 to 9 km during dust storms. Strong mixing below CBL creates dustiness over the observed area. The observed dust storm lasted for more than a sol significantly affecting the atmospheric structure and the planetary circulation, suggesting that the equatorward dust storm injected dust into the rising branches of the cell of Hadley circulation. Hence, though headily circulation dust mixing enhancement occurs in the middle atmosphere and the mid-level air temperatures rise. Further, we are trying to estimate the properties of the dust particle. The effective radius of the dust particle varies from 300 nm to 3000 nm. During the dust storm, air temperature increases up to 200 K. With the help of temperature data and retrieved water ice opacity data we have shown the formation of water ice clouds along the midlatitude of Mars. The formation of water ice clouds has been represented through the radiance data of availablelow-resolution images captured by the Visual Monitoring Camera (VMC).

Keyword: Mars Climate Sounder, Hadley Circulation, Convective Boundary Layer, Visual Monitoring Camera

Authors

Jyotirmoy Kalita
Department of Physics
Tingkhong College
Dibrugarh, Assam, India
jyotirmoy.physics@tripurauniv.in

Marylina Das
Department of Physics
Tripura university
Tripura, India

Suchibrata Saikia
Department of Physics
Dibrugarh University
India

Binita Pathak
Department of Physics
Dibrugarh University
India

Anirban Guha
Department of Physics
Tripura university
Tripura, India

I. HIGHLIGHT

1. Local dust storms injected dust into the rising branches of the cell of Hadley Circulation
2. Midlevel air temperature raised up to 200 K during the dust storm
3. Planetary circulation helps create the dustiness through variation of CBL
4. Air-born dust particles are of fine mode as well as coarse mode.

II. INTRODUCTION

Martian dust storm ranges from microscopic scale-like local (longitudinal axis >100km) to planet-encircling or like large dust storms with longitudinal axis >2000 km; (Martin and Zurek, 1993). The scientific community tried to understand the origin of dust storms and the planet's circulation pattern (Golitsyn, 1973; Gierasch and Goody, 1973). Large-scale dust storms like regional and Global dust storms used to last for more than a sol or even for weeks and microscopic scale-like local dust storms used to stay for more than half a sol. These dust events significantly affect the atmospheric structure and planetary circulation (Martin and Richardson, 1993; Smith et al., 2002; Wang et al., 2003; Cantor, 2007; Wang et al., 2007). Haberle et al. (1982); Strausberg et al., 2005;) suggested that the equatorward dust storm injected dust into the rising branch of the Hadley circulation. Hence, though Hadley circulation dust mixing enhancement occurs in the upper atmosphere, especially in the mesosphere, the mid-level air temperatures rise. So, accretion in the mid-level air temperature can be an indicator of dust storm occurrence. Moreover, regional dust storms generate thick haze over many areas. The haze may reach up to an altitude of 60 km and increase the normal dust opacity over the area (Cantor, 2007; Mishra et al., 2016). Water ice clouds and fog appeared in low-altitude topography on Mars without dust storms (Benson et al., 2010). The scientific community tried to find the dust movement initiated by dust storms and their impacts on the planet's circulation by opacity analysis (Heavens et al., 2011; Guzewich et al., 2015, 2017).

Based on the previous literature, Utopia Planitia has been considered the largest impact basin in the northern hemisphere of Mars. The Martian atmospheric dustactively influences the Martian climateand participates in the accretion ofthe albedo of the Martian surface due to the deposition of dust particles (Tang et al., 2021).

Previous studies already explored the combinedbehavior of thermal tides with water ice cloudsthat enriches the understanding furtherof the factors that involves to the formation of elevated temperature inversions. The previous literature adopted modeling studies to show thattropical effective temperature inversions may arise either dynamically from zonally modulated thermal tides (Wilson et al., 2003; Hinson and Wilson, 2000) or else radiatively from a dense water ice cloud layer (Colaprete and Toon, 2000, Haberle et al., 1999). During the dust storm, the planet possesses a huge temperature instability which further helps the formation of water ice clouds. In our present work, first, we investigate the atmospheric scenario during the local dust storms. Secondly, we investigate the temperature variation and opacities to see unreported dust activities throughout the planet. Thirdly, we investigate the temperature variation in relation to the water ice cloud from opacity data. Finally, we reported the whole atmospheric scenario during these 6 events of dust storms.

III. DATA AND METHODOLOGY

1. **MCS Data:** From September 24, 2006 (LS = 111°, MY 28), MCS observed the Martian limb, nadir, and off-nadir in nine broadband channels to detect dust, temperature, and condensates (McCleese et al., 2007, Kalita et al., 2021). Through limb observations with a moderate (5 km) vertical resolution from the surface to about 80 km altitude, we can extract vertical profiles of temperature (K), dust extinction (km-1; at 463 cm1 wavenumbers), and water ice extinction (km-1; at 843 cm1 wavenumbers) using MRO observations (Kleinböhl et al., 2009; Kalita et al., 2021). In the current study, we used MCS DDR data for MY 33–34, which are available in PDS by clicking the following link.

   https://pdsatmospheres.nmsu.edu/data_and_services/atmospheres_data/Mars/Mars.html Inside the MCS observational DDR data package, there is a.tab file that contains vertically integrated dust extinction. We might examine the overall observed dust opacity using the data on dust extinction. In the end, maximum atmospheric mass MCS retrievals in dusty conditions do not reach the surface (Guha et al., 2018, Kalita et al., 2021a, 2021b). As a result, the lowest retired point is used to determine the vertically integrated dust opacity while assuming a well-mixed profile. It should be emphasized that this supposition results in the extrapolated data for the limb seen. In order to study the variation in atmospheric characteristics, we used the density-scaled opacity technique described in Heavens et al. (2011) since it provides a seasonally and latitudinally variable opacity profile that is a good approximation of what might beappropriate. Density-scaled opacity is readily related to the aerosol mixing ratio. Also, the profile forwarded by Forget et al. (1999) cannot estimate the vertical dust distribution at certain latitudes and seasons. Moreover, density-scaled opacity helps understand a particular dust profile's radiative and dynamic importance (Heavens et al., 2011,Kalita et al., 2021a,2021b).

   In addition, we reported CBL height based on MCS data, computed the approximate height of the CBL based on MCS temperature data, and helped predict the intensity and height of the observed dust storm using MCS data (Kalita et al., 2021a, 2021b). The present work also focused on the dust and water ice opacity for the MCC observed events and the temperature profile.($dz\tau$ in km^{-1}; i.e., extinction per unit height due to dust or water ice) by atmospheric density ($\boldsymbol{\rho}$), i.e., $dz\tau$ / $\boldsymbol{\rho}$ in m^2 kg^{-1}. Through simulation, we estimated the necessary parameters using DDR-version 5 data (Kalita et al., 2021a, 2021b). To determine the particle's effective radius, we used the Mie theory. First, using information on water ice and dust extinction from the MCS, we compute the density scaled opacity. We computed the dust particle's effective radius using the data to estimate the dust's mixing ratio and the Mie theory.

$$mixing\ ratio(q_d) = \frac{4\rho_d(d_z\tau)r_{eff}}{3Q_{ext}\rho} \quad (1)$$

Also, the effective radius of water ice particle as,

$$mixing\ ratio(q_I) = \frac{4\rho_I(d_z\tau)r_{eff}}{3Q_{ext}\rho} \quad (2)$$

The Mie theory, as defined by Kleinböhl et al. (2009), where'reff' is the effective radius of particles, yields the value of 'Qext' as 0.78 for water ice particles and 0.350 in

the case of a dust particle. The ideal gas equation is used to calculate density from MCS data. The retrieved densities, $\boldsymbol{\rho}$I and $\boldsymbol{\rho}$D, have values of 900 kg m-3 and 3000 kg m-3, respectively. The particles' estimated effective radii range from 1.40 to 3.2 m. Additionally, we checked our effective radius calculations against the MCD GCM data for that specific event. In addition, we estimated the height of the CBL during the observation period and evaluated the static stability factor based on the temperature profile. The static stability value (S) is first plotted as a function of altitude. The observed S value should fall within the range of 1 and 2, and the matching height aids in estimating the CBL.

It is challenging to determine CBL height with accuracy. To calculate the CBL height, we take the S value of 1.5 into account. CBL height is determined using the occultation method by,

$$S = \frac{dT}{dZ} + \frac{g}{c_p} \quad (3)$$

Where g is the acceleration due to gravity $\frac{dT}{dZ}$ is the temperature gradient, and the Cp is the specific heat at constant pressure. Further, we subtracted the elevation of the area from occultation height to get the actual value of CBL (D) as,

$$D = Z_o + Z_e \quad (4)$$

2. **Mars Climate Database (MCD) Web Interface:** To estimate the effective radius of the dust particle we use MCD-based mixing ratio values. The web interface is as follows, http://www-mars.lmd.jussieu.fr/mcd_python/

   We put lat/long and altitude as input in the web interface and extracted the mixing ratio for the particular event. Further, we used the modeled value to calculate the effective radius of the particles. Also, based on the comparison between the detection wavelength and the radius of the particle we cautiously reported the mode of the particles.

3. **Visual Monitoring Camera Images:** To monitor the release of the Beagle-2 lander, the Visual Monitoring Camera (VMC) was included on Mars Express originally. The VMC was switched on again on 2007 and effectively used for almost a decade purely for outreach purposes. In 2016, collaboration with scientists from the University of the Basque Country UPV/EHU in Bilbao proved the scientific value of the data through studies of plumes (SANCHEZ-LAVEGAETAL et al., 2015). The Visual Monitoring Camera is aComplementary metal-oxide-semiconductor(CMOS) sensor that takes images by default in grayscale. Further, VMC is fitted with a Bayer Pattern filter so that color information may be extracted in post-processing (archives.esac.esa.int) The VMC low resolution images are processed to extract the luminosity value as follows,

   luminosity(a,b)=image(a,b,1)*0.299+0.587*image(a,b,2)+0.114*image(a,b,3) (5)

   After that we converted those DN number to radiance value to detect the cloud.

IV. RESULT AND DISCUSSION

The six local dust storms reported by Tiawnwen-1, in the year 2021 Tiwanwen-1 near midlatitude are as follows (*Qu et al., 2021*).

Table 1: Location and Solar Longitude Information for the Observed Events

Serial Number	Dust Storm Type	Solar Longitude (Degree)	Center Location (lat/long)
1	Local	13.1	47.0◦N, 101.2◦E
2	Local	13.8	52.0◦N, 107.2◦E
3	Local	21.3	61.3◦N, 130.1◦E
4	Local	21.8	64.3◦N, 121.1◦E
5	Local	27.1	54.6◦N, 104.9◦E
6	Local	27.4	53.4◦N, 107.2◦E

From the table we have the solar longitude and center location for the dust storms. The spreading area is reported >700,000 km^2. The area corresponds to ± 20 lat/long from the central coordinate represented in the table 1. We processed the Mars Climate Sounder (MCS) observed opacity data and found a satisfactory results. In figure 1 we may see the dust opacity for the corresponding events.

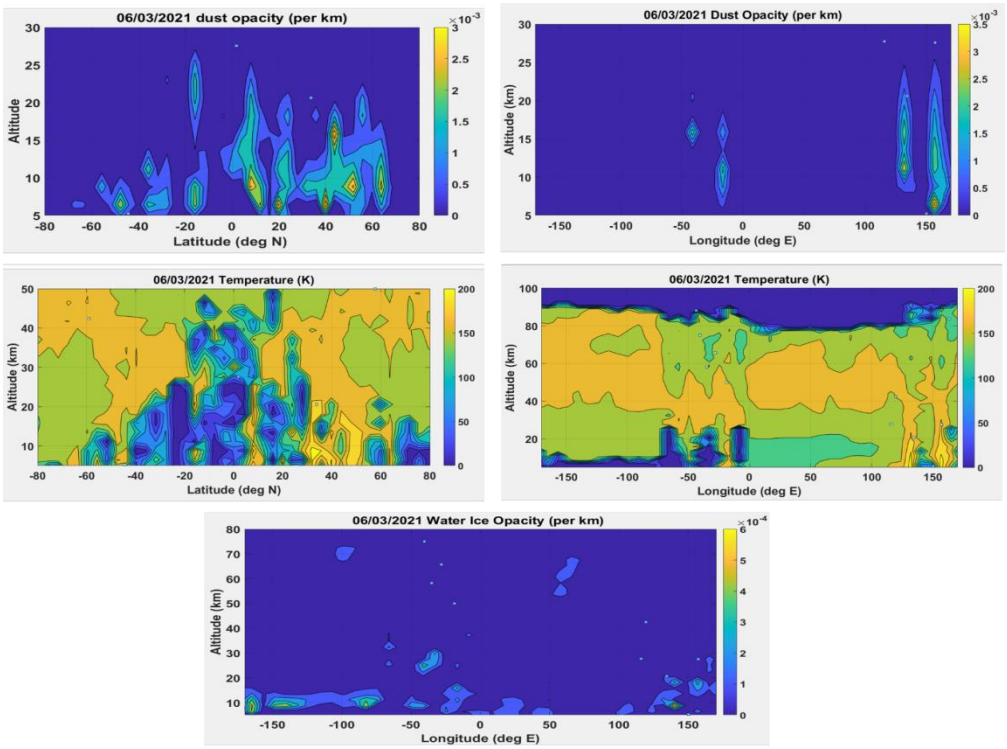

Figure 1: The figure illustrates the MCS observed latitudinally and longitudinally distributed dust and water ice opacity data as a function of altitude on 06/03/2021. In the longitudinal distribution, we can clearly see the two branches of temperature with a high value (~200 K) corresponds to dust opacity. That indicates the rise in temperature during

the dust storm. Also, a sudden increase in temperature below 20 km along -100 to -150 E results in the formation of a water ice cloud. Water ice opacity is $5x10^{-4}$ km^{-1} at the corresponding latitude.

The corresponding lat/long value is also verified with the represented opacity plot. On 06/03/2021 a high dust deposition is recorded over 52.0◦N, 130.2◦E. The mid-level air temperature also reaches up to 200K. Dust is injected up to a height of ~25 km. CBL is recorded as 8 km. Due to the rise in the height of CBL a strong mixing occurs between air and air-born dust. This redistribution creates dustiness over the Utopia Planitia. This largest basin of Mars possesses high albedo also due to the deposition of dust.

As we mentioned in figure 1 the water ice cloud formed over -100E to -150 E during the dust storm event due to an anomaly in temperature. Further, VMC images are represented to show the clouds. If we consider the tropical extension of Hadley circulation, we may indicate the branches with high-temperaturevalues where dust is injected from the lower atmosphere.

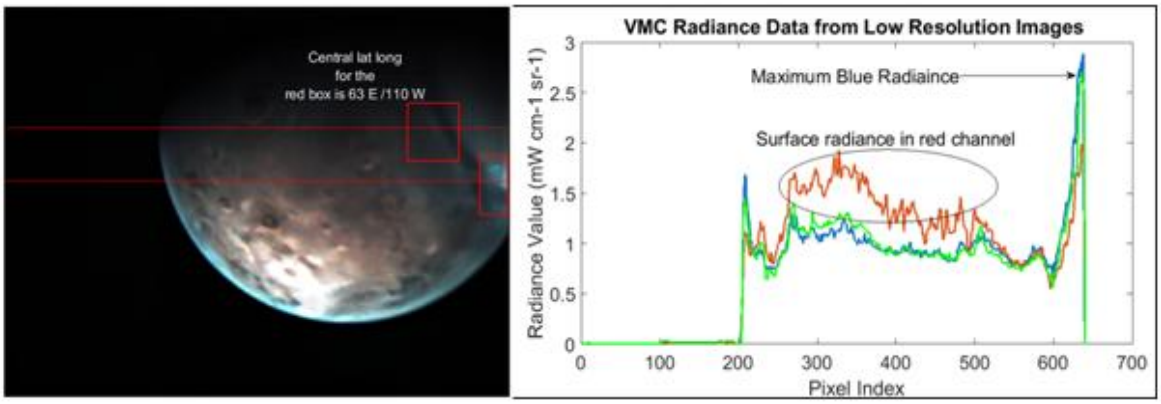

Figure 2: VMC low-resolution images with clouds. We took two transects (red line) to extract the radiance data. The radiance data confirms the presence of a water ice cloud.

We may see cloud structure over -100E to -150 E due to temperature anomaly as shown in figure 1. The red boxes illustrate the cloud portion of the low-resolution images. Further, the events have been processed through MCD to see the mixing ratio, wind pattern, and temperature. Temperature is further verified with the observed data.

We tried to consult MARCI's daily weather report to verify our events. Unfortunately, MARCI daily weather report is not available for that time period. Also, it is worth mentioning that we did not extract the reflectance value at the top of the atmosphere as we did in our previous paper (Kalita et al., 2021), because for that we need a deeper knowledge of VMC. In our present work, we presented low-resolution images to show the water ice cloud formed over other location during the events and we constrained ourselves up to the calculation of radiance value. We mainly focus on the temperature anomaly throughout the planet and their contribution for the formation of water ice clouds.

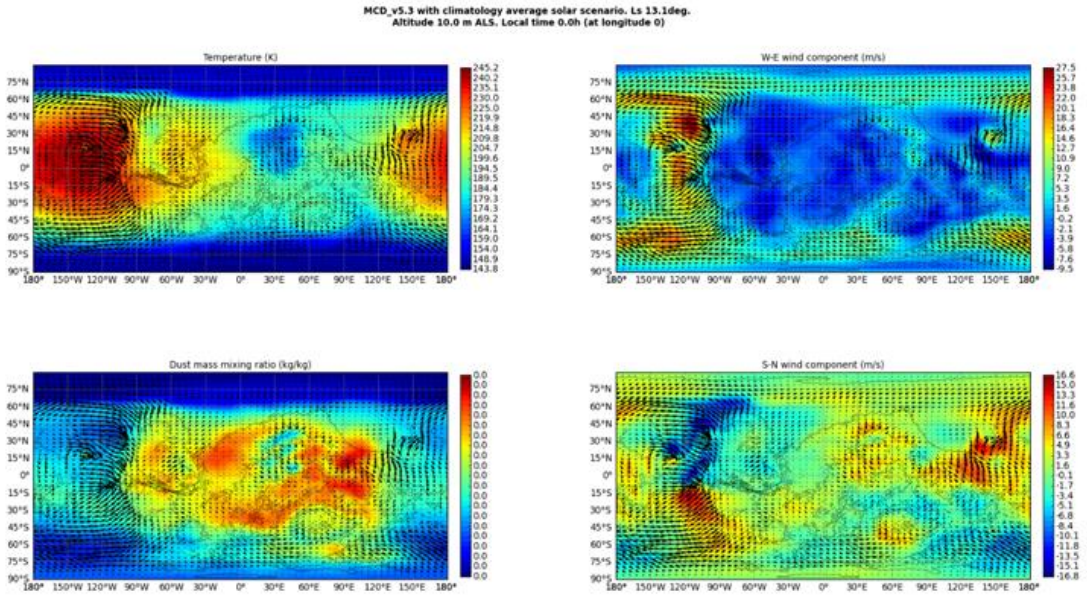

Figure 3 (a): MCD-based temperature, wind process, and mixing ratio plots. High westerlies drive the dust and are used to inject the dust into the rising branch of the Hadley circulation.

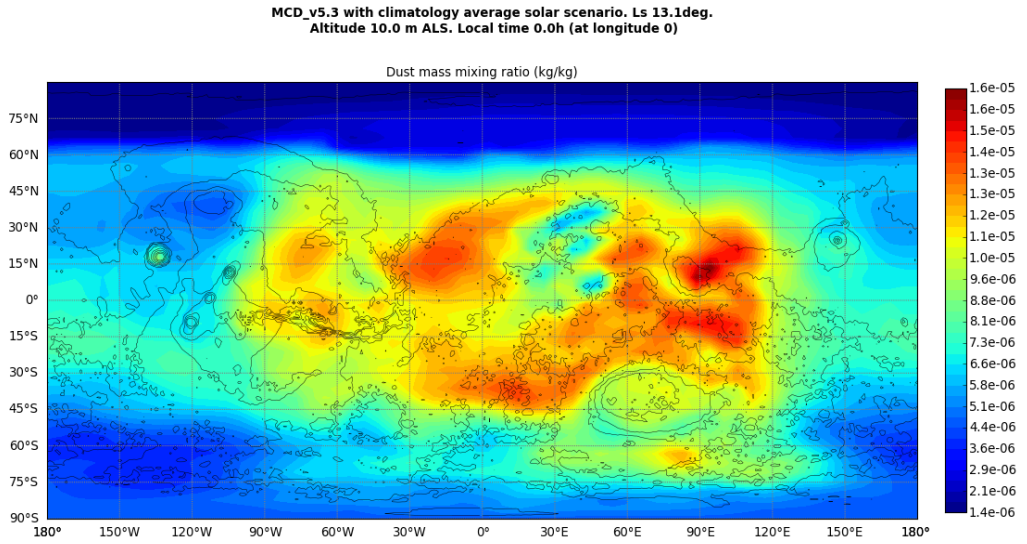

Figure 3 (b): The mixing ratio plot has been shown separately to illustrate how we used the mixing ratio data to extract the effective radius of the particles.

Similarly, on 08/03/2021 we analyzed the MCD and VMC data. High dust deposition is recorded over 52.0◦N, and 150.2◦E. The mid-level air temperature also reaches up to 200K. Dust is injected up to a height of ~20 km. CBL is recorded as 7.8 km. Due to the rise in the height of CBL a strong mixing occurs between air and air-born dust. This redistribution creates dustiness over the Utopia Planitia. High wind speed along W-E helps in the redistribution process. W-E wind varies from -35 to 35 m/s. Negative sign indicates the E-W wind flow over the observed area. Whereas, the S-N wind varies from -21 to 21 m/s. Both the events caries the evidence of coarse mode as well as fine mode particles.

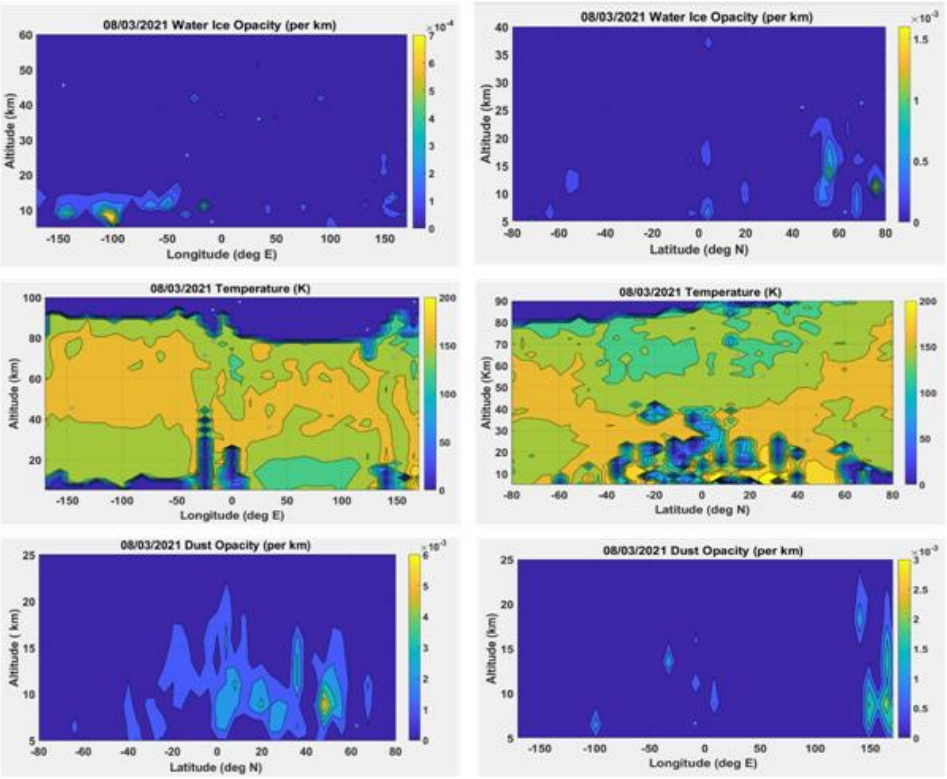

Figure 4: The figure illustrates the MCS observed latitudinally and longitudinally distributed dust and water ice opacity data as a function of altitude on 08/03/2021. In the longitudinal distribution, we can clearly see the two branches of temperature with a high value (~200 K) corresponds to dust opacity. That indicates the rise in temperature during the dust storm. Also, a sudden increase in temperature below 20 km along -100 to -150 E results in the formation of a water ice cloud. Water ice opacity is $7x10^{-4}$ km^{-1} at the corresponding latitude.

We concluded the mode based on the observed wavelength and effective radius of the particles. The effective radius during 06/03/2021 varies from 400 nm to 2100 nm whereas on 08/03/2021 the effective radius varies from 350 nm to 3000 nm. We already mentioned that we may extract the dust extinction (km-1) at 463 cm^{-1} wavenumbers, and water ice extinction (km-1) at 843 cm^{-1}wavenumbers. For the other four events, we have mentioned the details in table 2

Table 2: Illustrate the CBL Height,Wind Speed, and Temperature Data for the Local Dust Storm

Solar Longitude	CBL Height	Windspeed Maximum (M/S)	Maximum Temperature (K)
21.3	8.1	25	200
21.8	8.0	22	210
27.1	7.9	30	220
27.4	8.2	32	210

V. CONCLUDING REMARKS

1. During the local dust storms, the temperature used to rise over the observed area.
2. Rise in temperature and wind speed, convection as well as Variation in CBL helps the dust to be redistributed over the observed location.
3. Strong Dust mixing and injection of dust into the rising branch of Hadley circulation leave the area dusty after the local dust storm.
4. Throughout the planet temperature anomalies helps the formation of water ice cloud.
5. Bellow 15 km a sudden change in the temperature helps the formation of the clouds.
6. Effective radius of the particles varies from 300 nm to 3000 nm, further, helping the accretion of the Albedo value through strong mixing and redistribution of dust.

VI. ACKNOWLEDGMENT

All authors are thankful to the MCC data product team, ISRO for providing access to the required data for the present analysis (https://mrbrowse.issdc.gov.in/MOMLTA/). Also, the authors are thankful to the SSPO(ISRO) for funding the project with fund reference ISRO/SSPO/MOM- AO/2016-2019. A special thanks to Dr. Satadru Bhattacharya, Planetary Sciences Division, and Space Applications Centre (ISRO) for his constant support. Authors would like toacknowledge the Department of Science and Technology for a supporting fund to the Department of Physics, Tripura University through DST-FIST fund reference SR/FST/PSI-191/2014. The authors are also thankful to the MCS data providing team for publicly available data at PDS.

https://atmos.nmsu.edu/data_and_services/atmospheres_data/MARS/data_archive.html. The authors are also thankful to the VMC data team members for the publicly available dataPSA Introduction - PSA - Cosmos (esa.int).

REFERENCES

[1] Qu S, Li B, Zhang J, Wang Y, Li C, Zhu Y, Ling Z, Chen S. Evaluation and Analysis of Dust Storm Activity in Tianwen-1 Landing Area Based on the Moderate Resolution Imaging Camera Observations and Mars Daily Global Maps. Remote Sensing. 2022; 14(1):8. https://doi.org/10.3390/rs14010008
[2] Martin, L. J., and R. W. Zurek. 1993. An analysis of the history of dustactivity on Mars. J. Geophys. Res., 98(E2), 3221–3246.
[3] Gierasch, P.J. and R.M. Goody. 1973. A Model of a Martian Great DustStorm. J. Atmos. Sci., 30, 169–179.
[4] Golitsyn, G. S. 1973. On the Martian dust storms. Icarus, 18, 113 -1 19.
[5] Martin, T.Z., M. I. Richardson. 1993. New dust opacity mapping from VikingInfrared Thermal Mapper data. J. Geophys. Res., 98, 10,http://dx.doi.org/10.1029/93JE01044
[6] Smith, M.D. 2002. The annual cycle of water vapor on Mars as observed bythe thermal emission spectrometer. J. Geophys. Res. 107, 5115,doi.org/10.1029/2001JE001522.
[7] Cantor, B. A. 2007. MOC observations of 2001 planet-encircling dust storm.Icarus, 186, 60-96.
[8] Strausberg, M. J., H. Wang, M. I. Richardson, S. Ewald, A. D. Toigo. 2005.Observations of the initiation and evolution of the 2001 Mars global duststorm. J. Geophys. Res., 110 (E2).
[9] Wang, H. 2007. Dust storms originating in the northern hemisphere during thethird mapping year of Mars Global Surveyor. Icarus, 189, 325–343,doi:10.1016/j.icarus.2007.01.014.
[10] Wang, J.-S., & Nielsen, E. 2003. Behavior of the Martian dayside electrondensity peak during global dust storms. Planetary and Space Science,51(4-5), 329–338. https://doi.org/10.1016/S0032-0633(03)00015-

[11] HABERLE, R. M. 1986. Interannual Variability of Global Dust Storms onMars. Science, 234(4775), 459–461. doi:10.1126/science.234.4775.459
[12] Guzewich, S.D. et al., 2015. Mars Orbiter Camera climatology of textureddust storms. Icarus 258, 1–13, doi.org/10.1016/j.icarus.2015.06.023.
[13] Guzewich, S.D. et al., 2017. An investigation of dust storms observed with theMars Color Imager. Icarus, 289, 199–213,doi.org/10.1016/j.icarus.2017.02.020.
[14] Heavens, N. G. 2011. The vertical distribution of dust in the Martianatmosphere during northern spring and summer: Observations by the MarsClimate Sounder and analysis of zonal average vertical dust profiles. J.Geophys. Res., 116, E04003, doi:10.1029/2010JE003691.
[15] Guha, B. K., Panda, J., & Chauhan, P. 2018. Analysing some Martianatmospheric characteristics associated with a dust storm over the LunaePlanum region during October 2014. Icarus. doi:10.1016/j.icarus.2018.09.018
[16] McCleese, D. J. 2007. Mars Climate Sounder: An investigation of thermal andwate vapor structure, dust and condensate distributions in the atmosphere, andenergy balance of the polar regions, J. Geophys. Res., 112, E05S06,doi:10.1029/2006JE002790.
[17] Kleinböhl, A. 2009. Mars Climate Sounder limb profile retrieval ofatmospheric temperature, pressure, dust, and water ice opacity, J. Geophys.Res., 114, E10006, doi:10.1029/2009JE003358.
[18] Benson, J. L., D. M. Kass, A. Kleinböhl, D. J. McCleese, J. T. Schofield, andF. W. Taylor. 2010. Mars" south polar hood as observed by the Mars ClimateSounder. J. Geophys.Res., doi:10.1029/2009JE003554.
[19] Forget, F., F. Hourdin, R. Fournier, C. Hourdin, O. Talagrand, M. Collins, S.R. Lewis, P. L. Read, and J. P. Huot.1999. Improved general circulationmodels of the Martian atmosphere from the surface to above 80 km. J.Geophys. Res., 104, 24,155– 24,176.
[20] Michaels, T. I., and S. C. R. Rafkin. 2004. Large eddy simulation ofatmospheric convection on Mars. Q.J.R. Meteorol. Soc., 130, 1251– 1274,doi:10.1256/qj.02.169.
[21] Rafkin, S. C. R. 2009. A positive radiative-dynamic feedback mechanism forthe maintenance and growth of Martian dust storms. J. Geophys. Res., 114,E01009, doi:10.1029/2008JE003217.
[22] Spiga, A., F. Forget, S. R. Lewis, and D. Hinson. 2010. Structure anddynamics of the convective boundary layer on Mars as inferred from large-eddy simulations and remote sensing measurements. Q. J. R. Meteorol. Soc.,136: 414–428. DOI:10.1002/qj.563.
[23] Clancy, R. T. et al. 2000. An intercomparison of ground- based millimeter,MGS TES, and Viking atmospheric temperature measurements: Seasonal andinterannual variability of temperatures and dust loading in the global Marsatmosphere. J. Geophys. Res., 105(E4), 9553–9571.
[24] Melnik, O., & Parrot, M. 1998. Electrostatic discharge in Martian dust storms.Journal of Geophysical Research, 103(A12), 29,107–29,117.https://doi.org/10.1029/98JA0195
[25] Fisher, J. A., M. I. Richardson, C. E. Newman, et al. 2005. A survey ofMartian dust devil activity Mars Global Surveyor Mars Orbital Cameraimages. Journal of geophysical research, 110, E03004,doi:10.1029/2003JE002165.
[26] Jyotirmoy Kalita, Manoj Kumar Mishra, Anirban Guha,Martian limb-viewing clouds: A study based on MCC, MCS and MARCI observations,Planetary and Space Science,Volume 208,2021,105347,ISSN 0032-0633,https://doi.org/10.1016/j.pss.2021.105347.
[27] J. Kalita and A. Guha, "Initial investigation on different types of clouds observed by Mars Color Camera (MCC) from India's first Mars Orbiter Mission (MOM)," 2021 XXXIVth General Assembly and Scientific Symposium of the International Union of Radio Science (URSI GASS), Rome, Italy, 2021, pp. 1-4, doi: 10.23919/URSIGASS51995.2021.9560281

